Chinese Science Bulletin

Molecular modeling of the ion channel-like nanotube structure of amyloid β-peptide

JIAO Yong & YANG Pin†

Key Laboratory of Chemical Biology and Molecular Engineering of Ministry of Education, Institute of Molecular Science, Shanxi University, Taiyuan 030006, China

The ion channel-like nanotube structure of the oligomers of amyloid β-peptide (Aβ) was first investigated by molecular modeling. The results reveal that the hydrogen bond net is one of the key factors to stabilize the structure. The hydrophobicity distribution mode of the side chains is in favor of the structure inserting into the bilayers and forming a hydrophilic pore. The lumen space is under the control of the negative potential, weaker but spreading continuously, to which the cation selectivity attributes; meanwhile, the alternate distribution of the stronger positive and negative potentials makes the electrostatic distribution of the structure framework balance, which is also one of the key factors stabilizing the structure. The results lay the theoretical foundation for illuminating the structure stability and the ion permeability, and give a clue to elucidating the molecular mechanism of Alzheimer's disease (AD) and designing novel drugs to prevent or reverse AD at the root.

amyloid β-peptide, ion channel, nanotube structure, solvent accessible surface, electrostatic potential, Alzheimer's disease, molecular modeling

Alzheimer's disease (AD) is now the most common form of senile dementia. Just in 2006, AD affected about 4.6 million new patients worldwide[1]. As one of the defining pathological hallmarks of the disease[2], amyloid plaques consist mainly of amyloid β-peptide (Aβ), which is the centric molecule in the current study of AD pathology[3]. The ion channel hypothesis of AD proposes that Aβ converts its conformations and assembles into ion channel-like structures, which insert into plasma membranes and may lead to the leakage of membrane and the disruption of calcium homeostasis[4], and eventually result in the damage or death of neurons[5]. In 1993, Arispe et al.[6] first demonstrated the ability of $A\beta_{40}$ to form cation selectivity channels in an *in vitro* system, lipid bilayers. Subsequent experiments found the ion channel structures of $A\beta_{40}$ in diverse media, such as murine hypothalamic neurons[7], rat cortical[8] and hippocampal neurons[9]. In 2002, Perutz et al.[10] proposed a related nanotube structure of polyglutamine peptides, which is consistent with the X-ray and electron microscope data of the aggregates of Aβ and thus may be transplanted to the structure of Aβ aggregates. In 2006, Singer et al.[11] found the new evidence that the neurotoxic oligomers of Aβ can form the ion channel-like nanotube. Although a growing body of evidence supports the ion channel hypothesis, the high resolution structure of Aβ channel still remains unclear experimentally[5]. Based on the experimental data, the structure models of Aβ channel can be constructed by theoretical methods, which provides an alternative approach to insight into the formation of Aβ channel and its ion permeation mechanism. The nanotube structure of Aβ channel was first investigated by molecular modeling method in this work. The results reveal that the hydrogen bond net is one of the key factors to stabilize the

Received January 15, 2007; accepted April 16, 2007
doi: 10.1007/s11434-007-0220-2
†Corresponding author (email: yangpin@sxu.edu.cn)
Supported by the National Natural Science Foundation of China (Grant Nos. 30470408 and 20637010) and the Youth Foundation of Science and Technology of Shanxi Province (Grant No. 2006021009)

structure. The hydrophobicity distribution mode of the side chains is in favor of the structure inserting into the bilayers and forming a hydrophilic pore. The lumen space is under the control of the negative potential, weaker but spreading continuously, to which the cation selectivity attributes; meanwhile, the alternate distribution of the stronger positive and negative potentials makes the electrostatic distribution of the structure framework balance, which is also one of the key factors stabilizing the structure. The results lay the theoretical foundation for illuminating the structure stability and the ion selectivity and permeability, and give a clue to elucidating the molecular mechanism of AD and designing novel drugs for preventing or reversing AD at the root.

On the Insight II 2000 molecular modeling platform, the biopolymer module was employed to build and optimize the monomer and trimer models of the $A\beta_{40}$ nanotube structure under the constraint of X-ray diffraction data[10]. The homology and DelPhi module were used to calculate and analyze the properties of solvent accessible surface and electrostatic potential of the models, respectively. All of the calculations were carried out on the SGI workstation.

In Figure 1, the $A\beta_{40}$ with β-conformation winds in a tubular structure with two turns (20 residues each turn), in which the maximum (19) hydrogen bonds form successively between the carbonyl-oxygen atoms and the amide-hydrogen atoms of the peptide bonds on the adjacent backbones, and create the hydrogen bond net to stabilize the model; the side-chains extend alternately on either side of the backbone. The average diameter of the backbone is about 2.2 nm. Meanwhile, the main-chain conformational angels of the model are all in or near allowed regions of the Ramachandran plot; and the side-chain terminal atoms of the adjacent residues are also at the correct van der Waals distance (the average space about 0.36 nm)[10]. Driven mainly by the hydrogen bonds, $A\beta_{40}$ assembles into a trimer nanotube structure with the center of each subunit about 1 nm apart and the whole length about 3 nm along the direction of the tubular axis.

To quantitatively evaluate the hydrophobicity distribution of the nanotube structure, the solvent accessible surface (SAS) of $A\beta_{40}$ was calculated (Table 1), which referred to the qualitative distribution mode of the side chains proposed by Singer et al.[11], that is, the odd-numbered residues extending inward and the even-numbered ones outward (Figure 2). In Figure 2, the centric circular veins represent the water core, around which the rectangle frame represents the lipid bilayer environment. The main chains are rendered by black circles. The side chains are represented by the single-

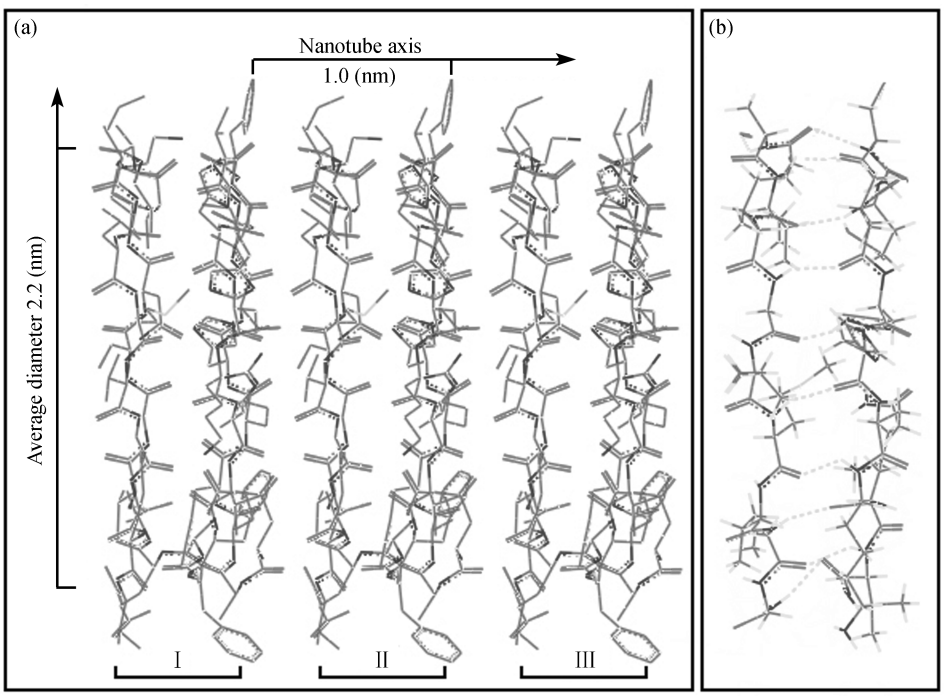

Figure 1 The structure of the nanotube model (a) and the hydrogen bond interaction between the main chains (b). The roman letters, I, II, III, represent an $A\beta_{40}$ subunit of the trimer, respectively.

Table 1 The comparison of the SAS properties of the parallel β-conformation with the tubular structure of $A\beta_{40}$

Surface area ($Å^2$)	Parallel β-conformation		Tubular structure		Change ratio (%)		P_a/N_a ratio			
	outer	inner	outer	inner	outer	inner	P_β	outer C_β	P_β	inner C_β
T_a	2918.78	2869.51	2560.62	1183.82	−12.27	−58.74	–	–	–	–
P_a	994.01	1508.54	676.44	587.46	−31.95	−61.06	0.52	0.36	1.11	0.99
N_a	1924.78	1360.98	1884.17	596.36	−2.1	−56.18	–	–	–	–

letter symbols of the residues which are numbered successively from the amino terminus to the carboxyl terminus. The odd-numbered residues extending inward to the water core are named the inner-residues, and the even-numbered residues extending outward to the bilayer are defined as the outer-residues. The hydrophobicity of the isolated residues at pH 7 is rendered by colors: red, hydrophobic; blue, hydrophilic; and green, in between. Based on the qualitative hydrophobicity of the isolated residues and the distribution of side chains mentioned above, Single et al.[11] proposed "the inner-the hydrophilicity, the outer-the hydrophobicity" distribution mode by comparing the number of the hydrophobic residues and that of the hydrophilicity together with the in-between residues. Actually, the hydrophobicity of the isolated residues may change with the difference of the primary structures, especially with the difference of the conformations in which they are located. The addition effect of the hydrophobic change of each residue impacts greatly upon the hydrophobic distribution of the $A\beta_{40}$ nanotube, and even results in the reversion of some local hydrophobic distribution. In this work, the influence of Aβ folding into nanotube structure on the hydrophobic distribution was taken into account by the SAS calculations; meanwhile, the uncertainty from the different ascription of the residues with the in-between hydrophobicity was eliminated (e. g. Singer et al. ascribed the hydrophilic residues together with the in-between ones to the same type), thus the hydrophobic distribution was evaluated quantitatively and more credibly.

The results of the SAS calculations (Table 1) reveal that the SAS values of each residue of the tubular structure all change (mainly reduce) compared with those of the parallel β-conformation; however, the whole hydrophobic property of the tubular structure still keeps "the inner-the hydrophilicity, the outer-the hydrophobicity" distribution mode. Especially, the hydrophobicity of the outer residues is enhanced markedly, which advantages the tubular structure to insert into the bilayers and exist stably.

Adopting the correspondence values of the parallel β-conformation as the benchmark, Table 1 shows that the total area (T_a) of the outer residues of the tubular structure decreases from 2918.78 to 2560.62 $Å^2$, and the T_a of the inner residues decreases prominently from 2869.51 to 1183.82 $Å^2$. The decrease of the outer T_a is about one-fifth of that of the inner T_a. The polar area (P_a) of the outer residues decreases from 994.01 to 676.44 $Å^2$, and the P_a of the inner residues decreases from 1508.54 to 587.46 $Å^2$. The nonpolar area (N_a) of the outer residues decreases from 1924.78 to 1884.17 $Å^2$, just decreasing by 2.11%; as a striking contrast, the N_a of the inner residues decreases from 1360.98 to 596.36 $Å^2$, with the decreasing extent up to 56.18%. Obviously, the SAS of the inner residues of the tubular structure shrinks dramatically compared with that of the parallel β-conformation, however, the ratio of P_a to N_a before folding almost equals that after folding, that is, 1.11 and 0.99, respectively, suggesting that the whole hydrophobicity of the inner residues is almost unaltered. But as far as the absolute values are concerned, the hydrophilicity of the inner residues decreases sharply to the extent slightly less than that of the hydrophobicity, and exhibits the reversional trend of the local hydrophobic distribution. Although the SAS of the outer residues shrinks too, the N_a is almost unchanged, and the ratios of P_a to N_a decrease from 0.52 before folding to 0.36 after folding, which implicates that the whole hydrophobicity of the outer residues is enhanced significantly. In addition, from the viewpoint of the comparison of the inner and the outer, the ratio of the P_a value of the outer to that of the inner is 1.15, suggesting that they are almost equal to each other; however, the ratio of the N_a value of the outer to that of the inner is 3.16, far apart to each other. So it reveals that the folding of $A\beta_{40}$ into the tubular structure enhances the outer hydrophobicity which favors the outer surface to insert into bilayers and the inner surface to accommodate the water core and ions permeation.

Figure 3(a) shows the isopotential distribution of the positive potential, +10 kT/e (red), and the negative po-

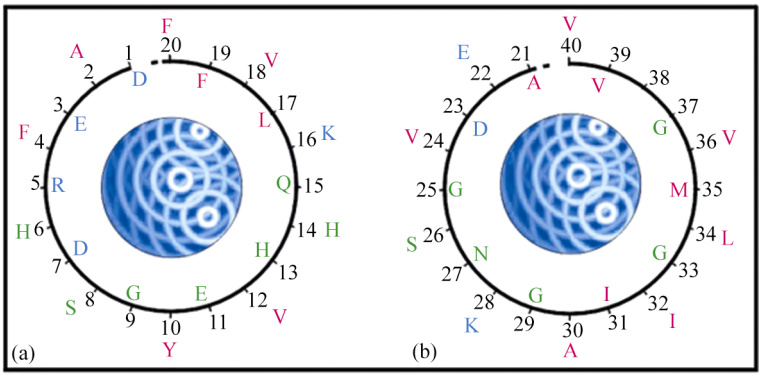

Figure 2 A schematic diagram of the side-chain distribution of the amino acid residues of $A\beta_{40}$ along the first (a) and the second turns (b) (the projection on the plane perpendicular to the direction of the nanotube axis).

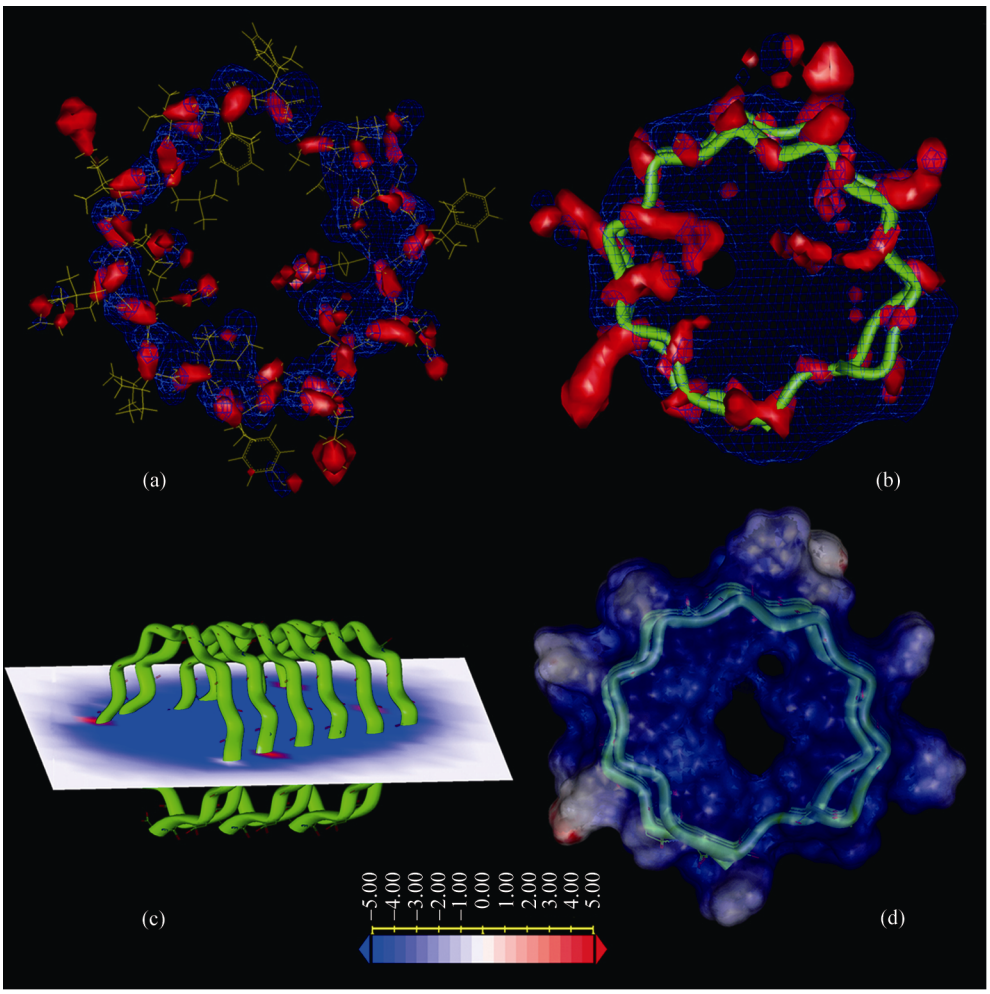

Figure 3 The electrostatic potential distribution (EPD) of the monomer and trimer of the tubular structure of $A\beta_{40}$. (a) The EPD of the backbone of the monomer structure; (b) the EPD of the pore of the monomer structure; (c) an isopotential section plane of the trimer nanotube; (d) the EPD of the van der Walls surface of the trimer nanotube.

tential, −10 *k*T/e (blue). In Figure 3(a), the potential distribution of the tubular structure is in the equilibrium and alternation mode for the positive and negative potentials with the range between $\geqslant$+10 and $\leqslant$−10 *k*T/e. The significance of this mode lies in avoiding the electrostatic repulsion by the excessive centralization of single type potential (positive or negative) and stabilizing the tubular structure. Figure 3(b) reveals the isopotential distribution of the positive potential, +5 *k*T/e (red), and the negative potential, −5 *k*T/e (blue). In Figure 3(b),

when the negative potential values decrease to below −5 kT/e, the negative isopotential surface joins in a continuous net; on the other hand, although the positive isopotential surfaces enlarge themselves to some extent, they are still isolated from each other. The lumen space is under the control of the continuous negative potential. Figure 3(c) is an isopotential section plane of the $A\beta_{40}$ trimer nanotube along the direction of the axis, which indicates that the inner space of the nanotube is under the control of about −5 kT/e negative potential. Figure 3(d) shows the electrostatic distribution which is mapped on the van der Walls surface of the tubular structure, and indicates that the inner residues and part of the main chain are under the control of the negative potential. All in all, the pore of the nanotube is under the control of the negative potential, which is consistent with the cation selectivity of Aβ channels in experiments[7].

In addition, we found that (detailed report in another paper) after zinc ion entering the negative-potential-controlled pore of the tubular structure, it can form stable chelate-ring by coordinating with the imidazole nitrogen atoms of the H13 residue and the carboxyl oxygen atoms of the E11 residue, which all have higher affinity with zinc ion. In this way, the zinc ion chelated with the pore occupies part of the pore space itself; on the other hand, the positive charges carried by the zinc ion electrostatically repulse the successive entering of other cations into the pore, so the pore is jammed and the permeation of the channel is blocked off. This result is consistent with the experimentally found blockage effect of zinc ion on the Aβ channels[7].

In a word, under the cooperative stabilization of the hydrogen bond net and van der Walls interaction, the nanotube structure of $A\beta_{40}$ forms the hydrophilic pore with the hydrophobicity distribution which advantages itself inserting into the lipid bilayers. The lumen space is under the control of the continuously negative potential, to which the cation selectivity attributes; the alternate distribution of the stronger positive and negative potentials makes the electrostatic distribution of the structure framework balance, which is another key factor stabilizing the structure. The results lay the theoretical foundation for illuminating the structure stability and the ion selectivity and permeability of the nanotube channel, and give a clue to elucidating the molecular mechanism of AD and designing novel drugs for preventing or reversing AD at the root.

1 Roberson E D, Mucke L. 100 years and counting: Prospects for defeating Alzheimer's disease. Science, 2006, 314(5800): 781－784

2 Selkoe D J. Alzheimer's disease: genes, proteins, and therapy. Physiol Rev, 2001, 81(2): 741－766

3 Masters C L, Cappai R, Barnham K J, et al. Molecular mechanisms for Alzheimer's disease: implications for neuroimaging and therapeutics. J Neurochem, 2006, 97(6): 1700－1725

4 Zheng X H, Wang L J, Zhang L, et al. Separation and analysis of the soluble trimer of $A\beta_{1-40}$ and its effects on the rise in intracellular calcium. Chin Sci Bull, 2006, 51(7): 830－838

5 Kagan B L, Azimov R, Azimova R. Amyloid peptide channels. J Membrane Biol, 2004, 202(1): 1－10

6 Arispe N, Rojas E, Pollard H B. Alzheimer disease amyloid β protein forms calcium channels in bilayer membranes: Blockade by tromethamine and aluminum. Proc Natl Acad Sci USA, 1993, 90(2): 567－571

7 Kawahara M, Arispe N, Kuroda Y, et al. Alzheimer's disease amyloid β-protein forms Zn^{2+}-sensitive, cation-selective channels across excised membrane patches from hypothalamic neurons. Biophys J, 1997, 73(1): 67－75

8 Furukawa K, Abe Y, Akaike N. Amyloid β protein-induced irreversible current in rat cortical neurons. Neuroreport, 1994, 5(9): 2016－2018

9 Qi J S, Qiao J T. Amyloid β-protein fragment 31-35 forms ion channels in membrane patches excised from rat hippocampal neurons. Neuroscience, 2001, 105(4): 845－852

10 Perutz M F, Finch J T, Berriman J, et al. Amyloid fibers are water-filled nanotubes. Proc Natl Acad Sci USA, 2002, 99(8): 5591－5595

11 Singer S J, Dewji N N. Evidence that Perutz's double-β-stranded subunit structure for β-amyloids also applies to their channel-forming structures in membranes. Proc Natl Acad Sci USA, 2006, 103(5): 1546－1550